

Using Switched Angle Spinning to Simplify NMR Spectra of Strongly Oriented Samples

Robert H. Havlin*, Gregory H.J. Park, Tanya Mazur and Alexander Pines

Materials Sciences Division, Lawrence Berkeley National Laboratory,
and Department of Chemistry, University of California,
Berkeley, California 94720

March 21, 2003

Abstract

This paper describes a method that manipulates the alignment director of a liquid crystalline sample to obtain anisotropic magnetic interaction parameters, such as dipolar coupling, in an oriented liquid crystalline sample. By changing the axis of rotation with respect to the applied magnetic field in a spinning liquid crystalline sample, the dipolar couplings present in a normally complex strong coupling spectrum are scaled to a simple weak coupling spectrum. This simplified weak coupling spectrum is then correlated with the isotropic chemical shift in a switched angle spinning (SAS) two-dimensional (2D) experiment. This dipolar-isotropic 2D correlation was also observed for the case where the couplings are scaled to a degree where the spectrum approaches strong coupling. The SAS 2D correlation of C_6F_5Cl in the nematic liquid crystal I52 was obtained by first evolving at an angle close to the magic angle (54.7°) and then directly detecting at the magic angle. The SAS method provides a 2D correlation where the weak coupling pairs are revealed as crosspeaks in the indirect dimension separated by the isotropic chemical shifts in the direct dimension. Additionally, by using a more complex SAS method which involves three changes of the spinning axis, the solid-like spinning sideband patterns were correlated with the isotropic chemical shifts in a 2D experiment. These techniques are expected to enhance the interpretation and assignment of anisotropic magnetic interactions including dipolar couplings for molecules dissolved in oriented liquid crystalline phases.

*corresponding author: rhavlin@speck.niddk.nih.gov, fax: 301-496-0825. Present address: Laboratory of Chemical Physics, National Institute of Diabetes and Digestive and Kidney Diseases, National Institutes of Health, Bethesda, Maryland 20892-0520

1 Introduction

Anisotropic interactions, such as dipolar couplings, have long provided a means for extracting structure from molecules using nuclear magnetic resonance (NMR)[1, 2]. Traditional structural methods in liquid state NMR measure dipolar couplings via the nuclear Overhauser effect (NOE) and use this information to solve three-dimensional structures in isotropic solutions[3, 4]. The NOE method in liquids quantifies the cross-relaxation rate due to dipolar coupling to extract $1/r^6$ distance information; methods in solid state NMR are able to directly measure the dipolar couplings with a $1/r^3$ dependence [5]. Although structure determinations using NOEs in isotropic solution have been fruitful, the $1/r^6$ distance constraints can be structurally limiting. Ideally, the $1/r^3$ dependence of dipolar coupling that is observed in solids could provide valuable structural constraints without the lower resolution typically seen in the solid state. The high-resolution observed in liquid state NMR is the result of isotropic molecular tumbling which averages the anisotropic interactions to zero. However, in the solid state the lack of isotropic motion gives rise to convoluted broad lines resulting from the presence of these anisotropic interactions. In oriented liquid crystals, anisotropic interactions, such as dipolar couplings, are only partially averaged. At least in simple samples, this partial averaging can provide well resolved, sharp lines that can yield valuable structural information.

The unique nature of the oriented liquid crystalline phase has provided an interesting realm for the study of anisotropic magnetic interactions in NMR [6, 7, 8]. These phases are aligned by an applied magnetic field while the individual molecules tumble about a magnetic alignment axis called a director and labeled \vec{n} in Figure 1. This molecular tumbling property

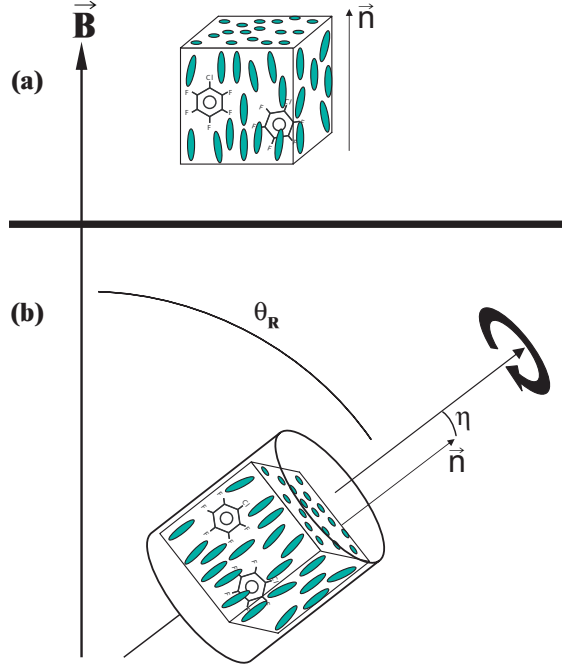


Figure 1: (a) Cartoon of the oriented liquid crystalline sample with the rods representing the liquid crystal molecules which align the solute molecule $\text{C}_6\text{F}_5\text{Cl}$ in the direction of the director \vec{n} . (b) The effect of sample spinning on the oriented sample. The angle θ_R denotes the spinning axis angle and η is the angle between the spinning axis and the director.

of liquid crystals yields an environment where anisotropic NMR interactions can be observed to a reduced degree while maintaining the high resolution found in the liquid state.

Recent advances in the availability of reliable liquid crystalline phases have catalyzed the measurement of dipolar couplings in routine protein structure determinations where they are referred to as ‘*residual* dipolar couplings’[8, 9]. The liquid crystalline systems commonly used for residual dipolar coupling determinations are intentionally prepared to only weakly align in the magnetic field. This weak alignment induces only weak dipolar couplings between directly bonded nuclei that can be easily interpreted as a small splitting ($\sim 5\text{-}10$ Hz). This is in contrast to strongly aligned systems where the spectrum becomes exponentially more complex with an increase in the strength and number of coupled spins.

However, strongly oriented systems can potentially provide valuable structural information via measurable couplings from nuclei separated by more than a single bond. If the long range couplings are measurable despite the increased spectral complexity, they provide strong geometrical constraints for use in three-dimensional structure determinations. Clearly, it is beneficial to utilize a more strongly orienting system if possible; however we must make efforts to simplify and facilitate interpretation of the increasingly complex dipolar coupled spectrum.

Examples of even simple molecules such as $\text{C}_6\text{F}_5\text{Cl}$ in a strongly aligned liquid crystal have observable ^{19}F - ^{19}F dipolar couplings on the order of kHz. When the chemical shift differences approach the coupling strength of nuclei, the dipolar couplings are no longer readily observed as splittings but are instead obscured in a complex spectrum such as in Figure 2a. This obscured spectrum no longer easily reveals the desired $1/r^3$ structural information. When strong homonuclear couplings between several nuclei exist, as in Figure 2a, the system is termed second order or strongly coupled and is a complex spin system that is difficult to both interpret and manipulate[5]. Although the dipolar couplings could be determined from a careful analysis of Figure 2a, determination of couplings in a slightly more complex spin system (with more spins and lacking symmetry) would be a grueling task. However, if the dipolar couplings are reduced to values smaller than their chemical shift differences, the useful structural information can be easily read from the spectrum, as shown in Figure 2b; this is what is termed a ‘first order’ type spectrum. The challenge in structure determination is the fact that the structurally important couplings are often weak and masked by shorter range dipolar couplings; thus we must attempt to introduce couplings as strongly as possible while maintaining interpretability. Currently, there exist a number of techniques that aid in

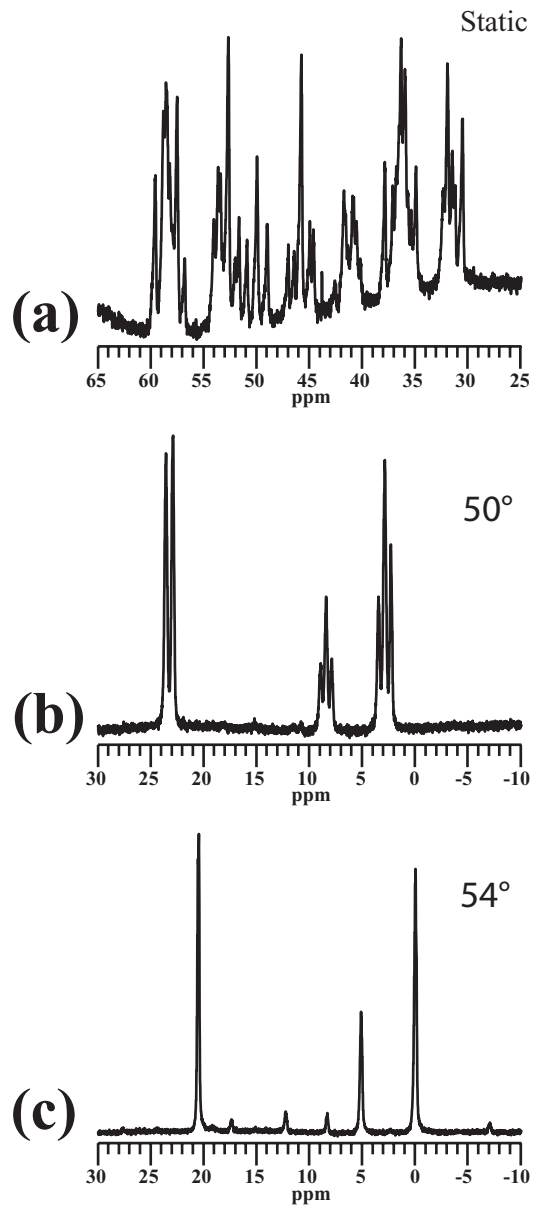


Figure 2: ^{19}F spectrum of $\text{C}_6\text{F}_5\text{Cl}$ in the nematic liquid crystal I52 15% w/w obtained (a) without sample spinning, (b) with sample spinning at 50° , and (c) under magic angle spinning. Spectra are shown in ppm from a reference frequency of 376.086 MHz.

the analysis and simplification of coupled systems. However, most of them have difficulty in dealing with second order type systems. One of the most promising groups of existing methods that are capable of dealing with second order systems are the heteronuclear local field experiments[10, 11]. Although heteronuclear dipolar couplings provide a first order type spectrum with the aid of homonuclear decoupling methods, the presence of more than one coupling can complicate interpretation. In order to keep the interpretation of the dipolar couplings tractable, their strength must remain minimal. This weak coupling requirement can often limit measurements to directly bonded atoms providing limited structural information in contrast to long range couplings that can yield excellent constraints in structure determinations.

In an effort to utilize more strongly dipole coupled liquid crystalline samples, several multiple pulse experiments have been developed which reduce[12] or even eliminate[13] homonuclear dipolar couplings to an extent which makes spectral interpretation viable. These methods perform well even in strongly coupled systems and possess only a modest scaling factor. Instead of employing RF pulses to reduce dipolar couplings, it is also possible to simplify dipolar couplings in liquid crystals by reorienting the alignment director whereby the intrinsic molecular motion performs the averaging[14, 15, 16, 17]. Director reorientation methods have no associated scaling factor and work well even in strongly coupled systems.

It has been shown that the alignment of the liquid crystal director can be readily manipulated with spinning according to the properties of the liquid crystal and the spinning angle[18, 19]. Depending upon the anisotropy of the diamagnetic susceptibility ($\Delta\chi$) of the liquid crystal, the director of the liquid crystalline phase will align parallel or perpendicular to the spinning axis according to the spinning angle with respect to the magnetic field,

θ_R , above a critical spinning rate [16]. For example, in a liquid crystalline sample with $\Delta\chi > 0$, as is the case with the sample studied in this work, the director aligns parallel to the spinning axis in the angle range of $0^\circ < \theta_R < 54.7^\circ$ and perpendicular in the range of $54.7^\circ < \theta_R < 90^\circ$. Therefore, in the appropriate spinning angle range, the alignment and thus the averaging of interactions in the sample can be controlled.

These scaled interactions can be assigned in a two dimensional (2D) switched angle spinning (SAS) experiment where the anisotropic interactions are first evolved at a given angle, and then the spinning axis is switched to the magic angle for detection of an isotropic dimension. In this manner the anisotropic interactions of the spins, that can be complex and difficult to interpret in a 1D mode, are now separated in the second dimension by their isotropic chemical shifts. Similar to previous work performed in solids [20, 21], in liquid crystals on first order dipolar couplings [17] and most recently in bicelles [22], the 2D SAS experiment provides a method for assigning dipolar couplings in liquid crystals using the isotropic chemical shift. In addition, a method that reveals the anisotropic interactions of individual spins in the liquid crystalline phase is also presented.

2 Experimental

To demonstrate the ability to scale a second order spectrum of an oriented liquid crystal sample, the ^{19}F NMR was observed for the small molecule perfluorochlorobenzene ($\text{C}_6\text{F}_5\text{Cl}$) dissolved in a nematic liquid crystal solvent. The second order ^{19}F spectrum of perfluorochlorobenzene (Sigma-Aldrich, St. Louis, MO) 15% w/w in the nematic liquid crystal I52 (EM Industries, Hawthorne, NY) is shown in Figure 2a. The liquid solute perfluor-

rochlorobenzene was dissolved in the liquid crystal I52 by slow mixing for 5 minutes. The liquid crystalline mixture was then placed in a 5 mm outer diameter ceramic rotor with rubber sealing gaskets[17].

The primary challenge of the experiment described is the ability to switch spinning angles rapidly during the course of the experiment. A switched angle spinning probe to be described elsewhere was used to evolve coherences at two angles. The probe used was a modified Chemagnetics (now Varian, Palo Alto, CA) HX probe fitted with an API Motion (now Danaher Motion, Washington, DC) stepping motor that was synchronized with the pulse programmer. The angle switching time in this experiment was 20 ms with a consistent angle accuracy of $< 0.1^\circ$.

The pulse program used to correlate the dipolar couplings with the isotropic chemical shifts was a modified SAS-COSY type experiment shown in Figure 4. Following an initial 90° pulse, the sample evolved while spinning off of the magic angle to allow for dipolar couplings in t_1 . The evolved anti-phase magnetization was then converted to in-phase z-magnetization by a $90_x - \tau / 2 - 180 - \tau / 2 - 90_{-y}$ where τ was constant and approximately $1/(4D)$ where D is the average dipolar coupling at the initial spinning angle. The spinning axis was then switched to the magic angle by triggering the motor controller. A 90° pulse was then applied to observe the isotropic signal. Following t_2 acquisition, the angle was switched back to the initial evolution angle for relaxation.

A second pulse sequence shown in Figure 7 was used to produce an alternate anisotropic-isotropic spectrum. This correlation was obtained with the liquid crystal directors aligned perpendicular to the spinning axis in t_1 and again with the directors aligned with the magic angle in t_2 . In this experiment, spinning sidebands resulting from the time dependent director

alignment in t_1 are correlated with the isotropic chemical shifts.

In the 1D experiments, the acquisition parameters were dwell= $30\mu s$, 8192 points giving a resolution of 4 Hz. The two dimensional experiments directly acquired with the acquisition parameters as with the 1D experiments and the second dimension having a dwell of $30\mu s$ and 1024 points giving a resolution of 32 Hz except for the 2D sideband correlations ($\theta_R \geq 54.7^\circ$) which had a dwell of $15\mu s$.

The magic angle was calibrated by a fit of the scaling of both the chemical shift and the dipolar couplings, in combination with the observation of the phase alignment transition (as evidenced in the spectrum) from parallel to perpendicular to axis of rotation.

3 Results

The motivation for developing methods to simplify and facilitate the interpretation of molecules in an oriented liquid crystalline phase is clearly shown in the one dimensional (1D) spectrum in Figure 2a. Although there is some resolution of peaks in the dipole coupled ^{19}F spectrum of oriented $\text{C}_6\text{F}_5\text{Cl}$, the three chemical shifts and ten dipolar couplings are not readily discerned. With 5 spins in this sample there is upper limit of 210 possible single quantum transitions (Z_1) from the expression[10, 23]:

$$Z_1 = \binom{2N}{N+1} = \frac{2N!}{(N+1)!(N-1)!} \quad (1)$$

where N is the number of spins- $\frac{1}{2}$. While symmetry may reduce the number of single quantum transitions significantly, many samples of interest do not have this benefit. A complete

analysis of spectra similar to Figure 2a requires a lengthy fitting routine that only converges to the correct spectral parameters δ^{aniso} , D_{ij}^{aniso} , and $S_{\alpha\beta}$ with appropriate initial conditions [24]. However, as the complexity of the spin systems increases, fitting routines become inadequate particularly when signal exists from multiple species in the spectrum or when the molecule is not rigid. Thus a spectroscopic alternative is necessary to study samples of more general interest.

The order parameter, $S_{\alpha\beta}$, describes the molecular motions of the molecules in the liquid crystalline phase and can be thought of as representing the average molecular orientation in the phase. Further details on the orientational order parameter can be found elsewhere [25, 26]. $S_{\alpha\beta}$ is defined by:

$$S_{\alpha\beta} = \frac{1}{2} \langle 3 \cos \theta_\alpha \cos \theta_\beta - \delta_{\alpha\beta} \rangle \quad (2)$$

where θ_χ ($\chi = x, y, z$) is the angle between the director and the molecular χ -axis and $\delta_{\alpha\beta}$ is the Kronecker delta function (1 if $\alpha = \beta$, 0 if $\alpha \neq \beta$). The dipolar coupling in the molecular frame is:

$$D_{ij,\alpha\beta}^{MOL} = -\frac{h\gamma_i\gamma_j}{2\pi r_{ij}^3} (3 \cos \theta_{ij,\alpha} \cos \theta_{ij,\beta} - \delta_{\alpha\beta}) \quad (3)$$

where $\theta_{ij,\chi}$ is the angle between the internuclear vector and the molecular χ axis, γ_i and γ_j are the magnetogyric ratios of the two nuclei, and r_{ij} is the internuclear distance. The remaining anisotropic component of the dipolar coupling, D_{ij}^{aniso} , now depends upon the order parameter matrix, $S_{\alpha\beta}$, and $D_{ij,\alpha\beta}^{MOL}$:

$$D_{ij}^{aniso} = \frac{2}{3} \sum_{\alpha\beta} S_{\alpha\beta} D_{ij,\alpha\beta}^{MOL} \quad (4)$$

In the case of $\text{C}_6\text{F}_5\text{Cl}$, we assume the molecule is rigid so that r_{ij} of Eq. (3) is constant. The chemical shift in an anisotropic phase is actually the sum of the isotropic and anisotropic chemical shifts:

$$\delta^{obs} = \delta^{iso} + \delta^{aniso} = \delta^{iso} + \frac{2}{3} \sum_{\alpha,\beta} S_{\alpha\beta} \delta_{\alpha\beta} \quad (5)$$

where $\delta_{\alpha\beta}$ are the elements of the chemical shift anisotropy tensor in the molecule fixed frame. Normally, both the isotropic and anisotropic J coupling would provide additional interactions for consideration in the spectral analysis. However, the J coupling was not observable in these experiments due to line widths resulting from field inhomogeneities and the anisotropic nature of the solvent. The J couplings have been previously reported as $J_{ortho,meta} = -21.3 \text{ Hz}$, and $J_{meta,para} = \pm 19.9 \text{ Hz}$ for the 3 bond J coupling and the longer range couplings were reported with values $\leq 6.3 \text{ Hz}$ [27]. These isotropic J coupling values should become apparent in the linear fits of the line splitting as a function of spinning angle discussed later. Although the isotropic J coupling would have an obvious contribution to any observed splitting, unfortunately, the anisotropic J coupling has a similar functional form as the dipolar coupling as described below in Eq. (7) and would arise as a systematic error in our analysis. Aside from the additional considerations the J coupling requires, if the order parameter can be determined, anisotropic information about the molecules can immediately be derived from the two observables δ^{obs} and (to first order) D_{ij}^{aniso} from the relationships in Eqns. (4) and (5). However, as the spin system becomes more complex, assignment is difficult and these relationships are less obvious.

Instead of employing a brute-force approach to interpretation of a spectrum such as in Figure 2a, the spectrum can be simplified first into more tractable portions. In addition to

the scaling of interactions resulting from $S_{\alpha\beta}$, the anisotropic components of D_{ij}^{aniso} and δ^{obs} can be further scaled if the director is aligned at an angle θ_R with the magnetic field[16]. With the liquid crystal directors reoriented, Eqns. (4) and (5) become:

$$\delta^{obs} = \delta^{iso} + \frac{1}{2}(3 \cos^2 \theta_R - 1)\delta^{aniso} \quad (6)$$

$$D_{ij}^{obs} = \frac{1}{2}(3 \cos^2 \theta_R - 1)D_{ij}^{aniso} \quad (7)$$

This scalability of the anisotropic interactions requires that the director axis is single-valued with respect to the magnetic field. Since the liquid crystal solvent I52 has the property of positive magnetic susceptibility anisotropy[28], the liquid crystal director aligns parallel to the spinning axis at angles $0^\circ < \theta_R < 54.7^\circ$ [16]. Thus by simply rotating the spinning axis to 50° with respect to the applied magnetic field, the dipolar couplings are scaled by the factor $\frac{1}{2}(3 \cos^2 50^\circ - 1)$, and a first order type spectrum is obtained. This reduction of strong second order dipolar couplings to simple first order couplings is readily seen in Figures 2a and 2b. At a spinning angle of 50° , the measured splittings are 250 Hz for the ortho-meta coupling and 195 Hz for the two meta-para couplings. Although scalar couplings could contribute to the observed splittings, the three bond scalar couplings were not observable, as shown in the isotropic spectrum of Figure 2c. In addition, the dipolar splitting of the single ^{19}F of the solvent liquid crystal was also observed with a splitting of 1085 Hz (not shown in Figure 2).

Figure 2c demonstrates how a second order spectrum can be reduced to an isotropic spectrum by spinning at the magic angle. With the nematic director aligned at the magic angle, the sample spinning provides the appropriate mechanism to align the liquid crystal director, and it is actually the uniaxial motion of the liquid crystal about the magic angle

that averages the dipolar couplings to zero. Since the liquid crystal motion is much faster than the 4.5 kHz spinning speed, the effectiveness of the averaging is much greater than could be obtained with spinning of a solid crystalline sample.

The observed ortho, para, and meta ^{19}F isotropic chemical shifts of perfluorochlorobenzene in I52 are 0.0, 5.1 and 20.5 ppm with intensity ratios of 2:1:2 referenced to 376.073058 MHz on a spectrometer where TMS (tetramethylsilane) ^1H resonates at 399.74179 MHz. The isotropic shifts reported were obtained from Figure 2c where the sample’s director is oriented at the magic angle. In addition to the isotropic resonances, small peaks appear in the spectrum that are due to spinning sidebands[29] occurring at the spinning frequency (ω_R). The spinning sidebands are the result of domains that are not aligned with the spinning axis and their anisotropic interactions then become time dependent with the rotor frequency. Due to the $\frac{1}{2}(3\cos^2\theta_R - 1)$ dependence of the aligning force, at exactly the magic angle, there is no favorable alignment direction[15]. Thus some liquid crystal domains begin to form a random powder-type alignment which results in spinning sidebands. These sidebands can be avoided by spinning at the magic angle for short times or at angles near the magic angle ($< 0.5^\circ$ away).

Figure 3 demonstrates the scalability of the dipolar couplings from second order to first order and ultimately to the isotropic spectrum. The isotropic spectrum obtained at 54° has the resonances indicated with arrows to the perfluorochlorobenzene molecule. The resonance furthest downfield arises from a single ^{19}F in the I52 liquid crystal solvent. Although this background solvent resonance has a measurable splitting at angles near the magic angle, the peak quickly broadens and shifts out of the spectral window to be folded into the opposite side causing a rolling baseline. The broadening of this peak is not the result of couplings to

the perfluorochlorobenzene but is instead the result of couplings to the numerous protons in the I52 liquid crystal molecules. Of more interest is what happens to the resonances from the perfluorochlorobenzene.

Examining the first order data in the angle range of 54° to 45° , we are able to extract some information about the anisotropic interactions. However, even in a 1D first order analysis, it is difficult to accurately assign the overlapping first order couplings. The dipolar coupling of the ortho peak suggests that $|D_{ortho,meta}^{aniso}|=2143$ Hz with an RMSD of 8 Hz as determined from a fit of the 1D first order doublet splitting to Eq. (7) which is a function of $P_2(\cos \theta_R)$, where $P_2(\cos \theta_R) = \frac{1}{2}(3 \cos^2 \theta_R - 1)$ is the second order Legendre polynomial. This linear fit has a intercept which corresponds to zero dipolar coupling of 18 Hz which is close to the isotropic J as was reported previously [27]. The meta and para fluorines were both pseudo-triplets; thus it is difficult to accurately determine the two different couplings present from a simple first order analysis. The 2D experiments described below will demonstrate how a second dimension helps to separate even these simple first order splittings. In addition to the perfluorochlorobenzene ^{19}F , the liquid crystal ^{19}F first order dipolar splittings could also be fit as a function of $P_2(\cos \theta_R)$ to give $|D_{LC}^{aniso}|=9885$ Hz with an RMSD of 50 Hz. In a similar fashion as with the dipolar couplings, the chemical shift could also be fit using Eq. (6) to give δ^{iso} and δ^{aniso} . The anisotropic contributions to the shift, δ^{aniso} , from the 1D data were fit to Eq. (6) to give the following values with the RMSD values in parentheses: $\delta_{LC}^{aniso}=12805$ (62), $\delta_{ortho}^{aniso}=10045$ (49), $\delta_{para}^{aniso}=12102$ (59), and $\delta_{meta}^{aniso}=10573$ (52) Hz. The isotropic shift values from the intercept of this fit were: δ_{LC}^{iso} 16332, $\delta_{ortho}^{iso}=7713$, $\delta_{para}^{iso}=1921$ and $\delta_{meta}^{iso}=0$ Hz. These values will be addressed again and compared to the results from the 2D correlations. As mentioned earlier, any significant anisotropic J coupling contribution

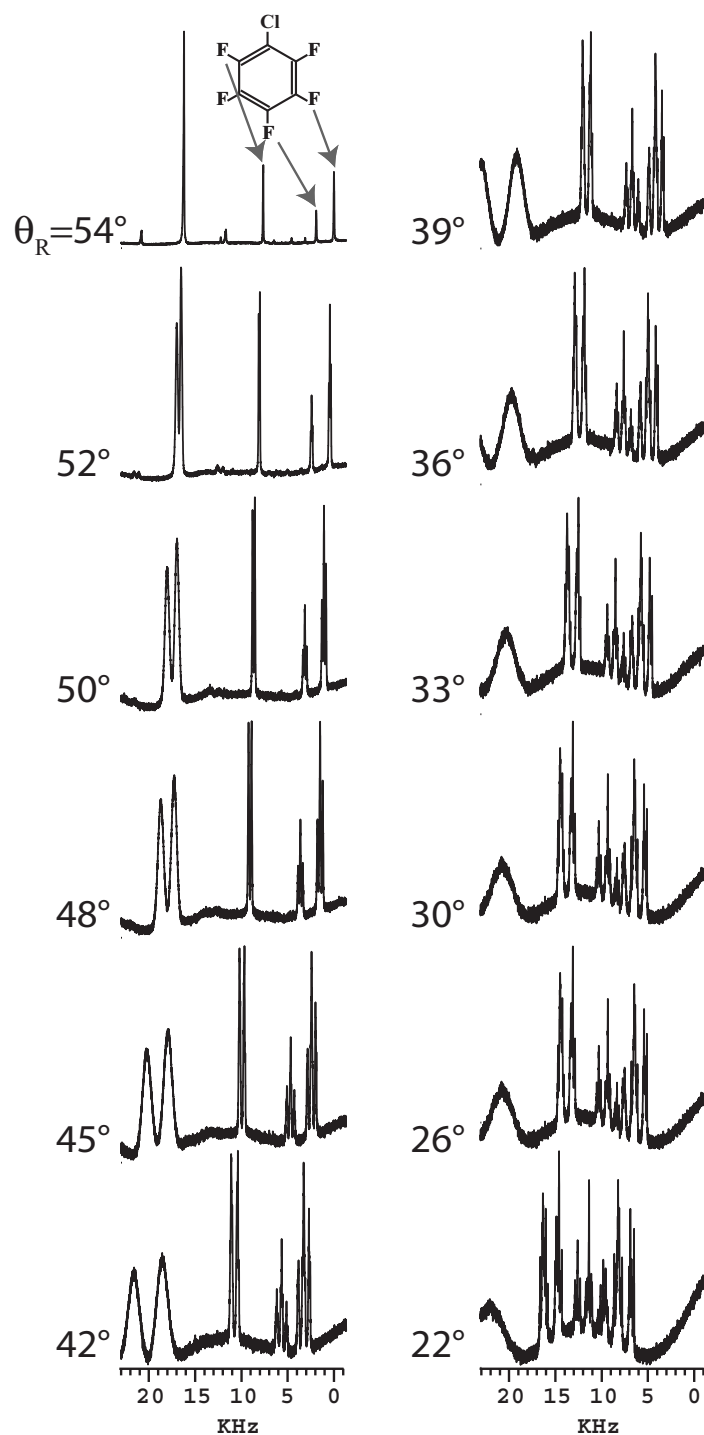


Figure 3: ^{19}F 4 kHz spinning spectra of perfluorochlorobenzene in I52 with the spinning axis at the angle, θ_R , relative to the field as indicated in the figure.

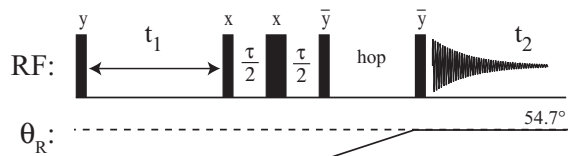


Figure 4: SAS-COSY pulse sequence used in Figures 5 and 6. The upper half shows the radiofrequency pulses with the narrow blocks representing a 90° pulse and the wider block representing a 180° pulse. The lower half shows how the spinning angle, θ , changes during the pulse sequence with direct detection at the magic angle (54.7°).

would cause a systematic error to the fit of the anisotropic dipolar coupling, in addition, angle errors due to inaccuracies in the motor controller system could also introduce errors in the linear regression data.

Couplings to ^{19}F beyond the nearest neighbor ^{19}F become apparent at angles smaller than $\sim 50^\circ$. At spinning angles of $\sim 40^\circ$, the spectral complexity begins to make interpretation difficult. Using the angle analysis of Figure 3 the spinning angles of 50° and 40° were selected to study in a SAS-2D mode with hopes that they would provide an example of both first- and second order couplings correlated with an isotropic dimension.

3.1 2D Dipolar-Isotropic Correlations ($\theta_R \leq 54.7^\circ$)

The goal of this work was to examine how an isotropic dimension might provide additional information in what are inherently strongly dipolar coupled systems using a SAS-2D correlation. In this simple sample we wish to demonstrate the feasibility of observing cross-peaks to facilitate dipolar coupling assignments. Using the pulse sequence of Figure 4 on the same sample as shown in Figure 2, $\text{C}_6\text{F}_5\text{Cl}$ in I52, the first order 2D correlation of Figure 5 was obtained. The angle θ_R for the initial dipolar evolution was set to 50° to scale the

couplings sufficiently to obtain a readily interpretable first order spectrum. In Figure 5 the observed crosspeaks of different spins reveal not only the coupled spins but also the coupling values in a clearly separated manner. The furthest downfield ortho ^{19}F has an observable crosspeak only with the upfield meta ^{19}F , and the single midfield para ^{19}F has an observable crosspeak to two neighboring meta ^{19}F . The para-meta crosspeaks are not as strong due to the one-half intensity of the para peak; however the cross-peak on the right of the spectrum clearly shows the expected +/- pattern. The +/- pattern of the crosspeaks results from the modulation of the transferred coherence as $\sin(Dt_1)$ instead of the familiar in phase $\cos(Dt_1)$. The sign difference also helps to clearly separate the two overlapping doublets of the meta and para ^{19}F which are difficult to distinguish in the 1D spectrum. By utilizing the separation provided in Figure 5, the observed couplings at the crosspeaks were determined to be $D_{ortho,meta}^{obs} = 272$ and $D_{meta,para}^{obs} = 181$ Hz. The measured value of $D_{ortho,meta}^{obs}$ from the 2D data spectrum is within experimental error of the linear predicted 1D data. Since only the $D_{ortho,meta}^{obs}$ was readily measurable from the 1D data we do not compare the value of $D_{meta,para}^{obs}$.

Another notable point in Figure 5 is the fact that there is a slight shift from the isotropic chemical shift values in the indirect dimension due to the non-zero contribution from the chemical shift anisotropy according to Eq. (6). By comparing the resonance frequencies of the diagonal peaks in the isotropic and anisotropic dimensions, the CSA contributions were fit to Eq. (6) to give values within the error of the measurements from the 1D data. Although the isotropic shift, δ^{iso} , was directly determined from the isotropic dimension, the values were identical to those fit in the previous section and observed in Figure 2c. In combination with a quantitative determination of the order parameter of the liquid crystalline phase, structural

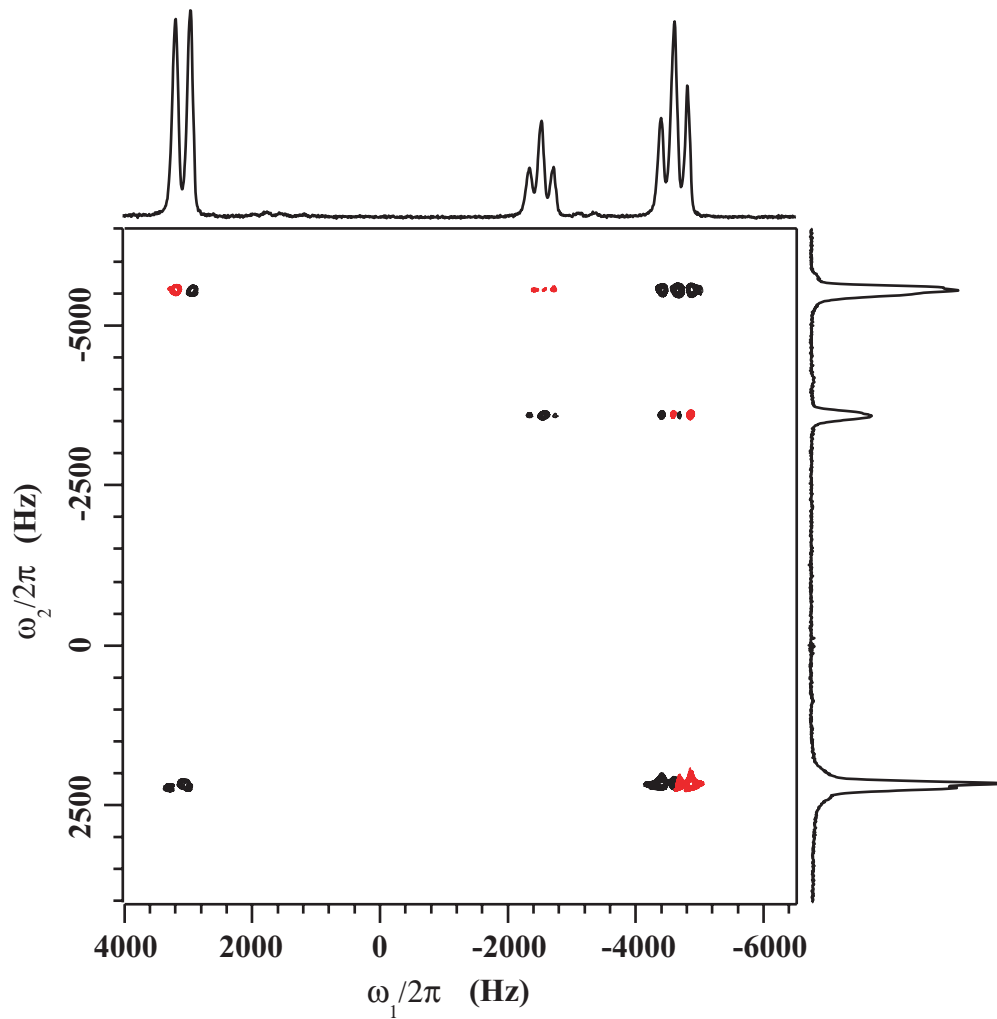


Figure 5: ^{19}F SAS-COSY 2D spectrum of $\text{C}_6\text{F}_5\text{Cl}$ in the liquid crystal I52 obtained with the pulse sequence of Figure 4. The sample was spinning at 4 kHz and switching angles (θ_R) from 50° in ω_1 and the magic angle in ω_2 .

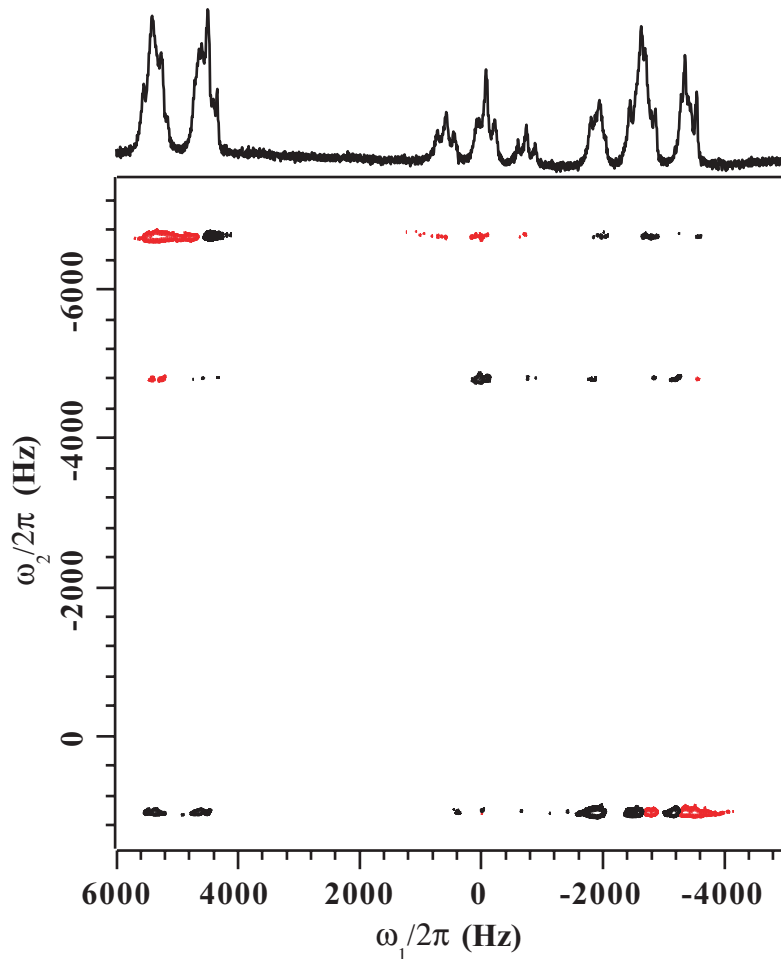


Figure 6: ^{19}F SAS-COSY 2D spectrum of $\text{C}_6\text{F}_5\text{Cl}$ in the liquid crystal I52 obtained with the pulse sequence of Figure 4. The sample was spinning at 4 kHz and switching angles (θ_R) from 40° in ω_1 and the magic angle in ω_2 .

information could be obtained readily from the CSA and dipolar couplings as determined from the crosspeaks in this method. Overall, Figure 4 successfully assigns the first order couplings to the appropriate isotropic chemical shifts.

Although the analysis of the first order couplings could be easily assigned in Figure 5, the correlation of the second order spectrum obtained at 40° with the isotropic spectrum, shown in Figure 6 demonstrates how rapidly the spectrum becomes difficult to interpret. Again, using the pulse sequence of Figure 4, the characteristics of the first order spectrum

can clearly be seen as a doublet and two triplets with some sub-structure due to coupling beyond the nearest neighbor ^{19}F . This can be seen directly by the appearance of additional crosspeaks where there were previously none in the first order correlation; however it is difficult to quantitatively determine the strength of all of the couplings in the sub-structure. Although the value of τ could easily be adjusted to emphasize a particular strength coupling in the correlation, we instead used a value determined by the average of the three largest perfluorochlorobenzene couplings.

Adding to the difficulty in the interpretation of the crosspeaks is a phase distortion which most likely arises because of ill-defined pulse angles due to the near second order type coupling system[5]. It should be noted that the 1D spectrum shown at the top of the 2D contour plot is not a projection but instead is the 1D spectrum obtained under the SAS-2D conditions. However, in both the first order and second order 2D correlations, the indirect evolution is clearly separated by each of the isotropic chemical shifts.

3.2 2D Sideband Correlations ($\theta_R \geq 54.7^\circ$)

The previous section described a method for obtaining correlations where the director alignment is maintained parallel to the spinning axis while the director is manipulated between the magic angle and 0° . However, the director alignment in this liquid crystal can also be reoriented to the perpendicular phase via spinning the sample at angles $54.7^\circ < \theta_R < 90^\circ$ to provide spinning sidebands of the anisotropic interactions as shown in Figure 8a. In this spectrum the spinning sidebands of the ^{19}F appear at $2\omega_R$ for all of the resonances. The spectrum demonstrates how the directors of the sample have oriented at 90° with respect

to the spinning axis, and the signal is modulated according to Eq. (8). Instead of a simple scaling of the interactions with a change in θ_R as in Eq. (7), the signal now has a time dependence of the form [30, 31]:

$$\begin{aligned}
S(t, \theta_R, \eta, \psi, \omega_R) &\propto \frac{1}{2}(3 \cos^2(\theta_{Lab}(t)) - 1) \\
&\propto \frac{1}{4} (3 \cos^2 \theta_R - 1) (3 \cos^2 \eta - 1) \\
&\quad + \frac{3}{4} \sin^2 \theta_R \sin^2 \eta \cos(2\omega_R t + 2\psi) \\
&\quad + \frac{3}{4} \sin 2\theta_R \sin 2\eta \cos(\omega_R t + \psi)
\end{aligned} \tag{8}$$

which for $\theta_R=54.7^\circ$ reduces to:

$$\begin{aligned}
S(t, \theta_R, \eta, \psi, \omega_R) &\propto +\frac{1}{2} \sin^2 \eta \cos(2\omega_R t + 2\psi) \\
&\quad + \frac{1}{\sqrt{2}} \sin 2\eta \cos(\omega_R t + \psi).
\end{aligned} \tag{9}$$

Thus, when spinning this sample at an angle slightly larger than the magic angle, η changes from zero to 90° , the $\cos(\omega_R t)$ vanishes, and all of the anisotropic interactions are modulated by $\cos(2\omega_R t)$ and scaled by a factor of $\frac{1}{6}$. Then interactions can be determined from the analysis of the sideband intensities in a manner similar to that used in the solid state[32]. However, the sidebands tend to overlap, making this type of analysis difficult.

A method to aid in resolving the overlapping sidebands of Figure 8a would be to correlate a spinning sideband spectrum with an isotropic spectrum in a SAS experiment similar to the one described in the previous section. In order to perform this type of experiment the directors must be reoriented parallel to the spinning axis to yield an isotropic dimension.

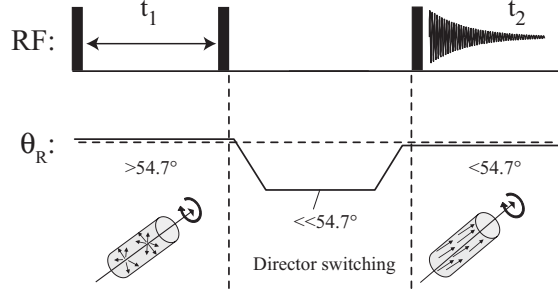


Figure 7: Director reorienting pulse sequence which first evolves with the directors aligned perpendicular to the spinning axis in t_1 near the magic angle and then with the director parallel to the spinning axis in t_2 also near the magic angle. The horizontal dashed line represents $\theta_R = 54.7^\circ$.

Assuming the director reorientation is rapid, this can be accomplished by the SAS experiment shown in Figure 7. The experiment begins with the directors aligned perpendicular to the spinning axis, and t_1 is evolved. Then the angle is switched to 50° to rapidly orient the directors parallel to the spinning axis. Finally, the angle is switched again to slightly less than the magic angle to observe the isotropic spectrum for the direct t_2 dimension. Following acquisition, the spinning axis is switched back to 55° for relaxation and reorientation to the perpendicular phase. The perpendicular t_1 evolution is obtained at an angle of 55° to keep resonances sharp since they otherwise broaden due to other terms arising from a non-zero value of $P_2(\cos \theta_R)$.

The 2D correlation obtained using the sequence of Figure 7 is shown in Figure 8b. The sideband patterns are clearly separated by their isotropic chemical shifts. Now the anisotropic information encoded in the sidebands can be fit easily. However, the anisotropic information is actually a combination of CSA and dipolar couplings as scaled by the factor $P_2(\cos \theta_R)$ and modulated according to Eq. (9). In order to separate the contributions from these two interactions, RF pulses could be applied during the t_1 evolution to refocus the chemical shift.

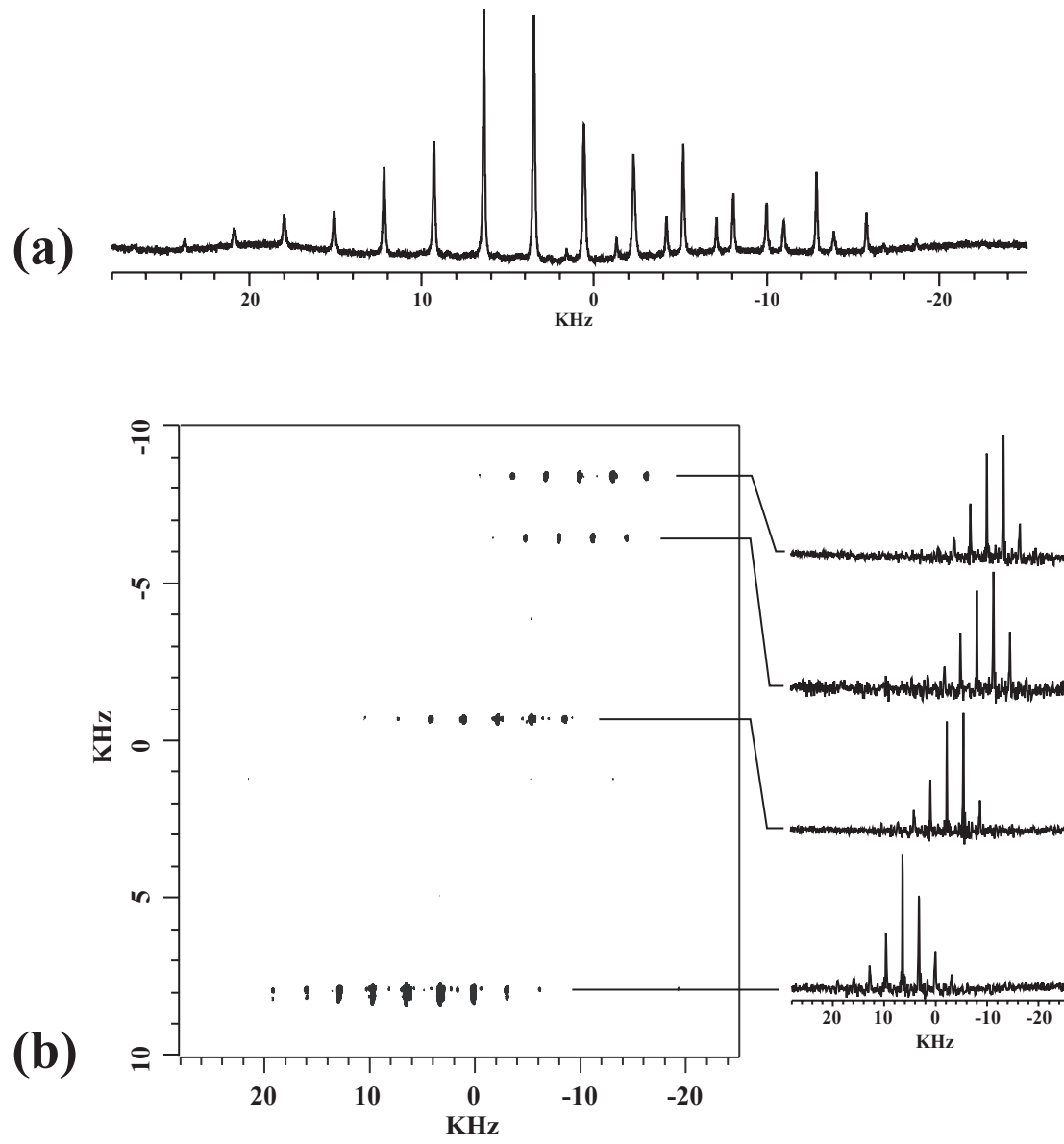


Figure 8: (a) The 1D perpendicular phase spinning sideband spectrum with $\theta_R=55^\circ$. (b) 2D SAS isotropic-sideband correlation generated with the pulse sequence in Figure 7.

Alternatively, a homonuclear decoupling sequence such as Lee-Goldburg[33] could be applied to remove the homonuclear couplings and leave the chemical shift. Although no separation of the anisotropic interactions was performed, the sideband-isotropic correlation principle is demonstrated in Figure 8b. To the right of the 2D contour plot are 1D slices showing the sideband patterns for each spin. The furthest downfield resonance again corresponds to the liquid crystal background and has significantly more intensity than the three resonances from the perfluorochlorobenzene. In this case we expect many sidebands for all of the resonances in the sample due to the presence of both large dipolar couplings as well as large ^{19}F CSAs.

Although this 2D correlation is of limited use in the case of this sample, quantitative determination of the CSA could be performed for samples containing natural abundance ^{13}C under ^1H decoupling where only the CSA contributes to the sideband pattern. This type of experiment could prove extremely valuable for samples such as ^{13}C labeled proteins where the CSA could aid in structure determination [34, 35, 36].

4 Conclusions

With experimental ease, the second order dipole coupled spectrum can be reduced to a first order spectrum, and then the couplings can be assigned via their isotropic chemical shifts. This method takes the laborious task of assigning the numerous peaks in the second order spectrum and reduces it to the simple task of reading off crosspeaks in the 2D SAS correlation. Some would argue that much of the valuable structural information has been lost by reducing the couplings to first order; however this method has the flexibility to perform as much or as little averaging as the experimenter desires. By performing a SAS correlation

between 0° and the magic angle, all of the spectral complexities of the non-spinning case may be recovered.

These methods are applicable to many types of liquid crystals whether they are strongly or weakly oriented, and it is not limited to liquid crystals whose directors can be aligned with sample spinning. For example, samples that achieve alignment through polymer alignment can simply be reoriented by moving the polymer alignment axis [19] in order to correlate dipolar couplings in a wider variety of samples. In addition, this method can be implemented to study more complex spin systems with a degree of flexibility that greatly facilitates spectral analysis. There exist several possible opportunities to utilize switched angle correlation experiments to obtain valuable structural insight into aligned samples.

Implementation of the techniques described here may be beneficial for the interpretation of dipolar couplings and CSAs in liquid crystalline phases. A technique where correlations are performed at successively smaller angles would provide insight into the details of how a first order spectrum transitions into a second order spectrum.

A further application of this technique is to explore more interesting systems. Although the sample investigated here is a relatively simple one, recent demonstrations with oriented bicelle phases[22, 37] indicate that this method could be applied to more challenging systems such as membrane proteins. This technique could provide the great benefit of maintaining the isotropic chemical shift for assignment while having the flexibility to scale the dipolar couplings for optimal structural interpretation in a single sample.

5 Acknowledgements

We wish to thank Dr. Jamie Walls for his helpful discussions. R.H.H. acknowledges the National Science Foundation for a pre-doctoral fellowship. This work was supported by the Director, Office of Science, Office of Basic Energy Sciences, Materials Science and Engineering Division, U.S. Department of Energy under Contract No. DE-AC03-76SF00098

References

- [1] D. M. Grant and R. K. Harris, editors. *Encyclopedia of Nuclear Magnetic Resonance*, volume 1-9. Wiley, 2002.
- [2] D. D. Laws, H. M. L. Bitter, and A. Jerschow. Solid-state NMR spectroscopic methods in chemistry. *Angew. Chem., Int. ed. Eng.*, 41(17): 3096–3129, 2002.
- [3] K. Wuthrich. *NMR of proteins and nucleic acids*. Wiley, New York, 1986.
- [4] J. Cavanagh, A. G. Palmer, W. Fairbrother, and N. Skelton. *Protein NMR Spectroscopy: Principles and Practice*. Academic Press, 1996.
- [5] R.R. Ernst, G. Bodenhausen, and A. Wokaun. *Principles of Nuclear Magnetic Resonance in One and Two Dimensions*. Clarendon Press, Oxford, 1987.
- [6] J. W. Emsley and J. C. Lindon. *NMR Spectroscopy Using Liquid Crystal Solvents*. Pergamon Press, Oxford, 1975.

- [7] A. D. Buckingham, E. E. Burnell, and C. A. Delange. Determination of nuclear magnetic shielding anisotropies of solutes in liquid-crystal solvents. *J. Am. Chem. Soc.*, 90(11): 2972, 1968.
- [8] E. de Alba and N. Tjandra. NMR dipolar couplings for the structure determination of biopolymers in solution. *Prog. Nucl. Magn. Reson. Spectrosc.*, 40(2): 175–197, 2002.
- [9] N. Tjandra and A. Bax. Direct measurement of distances and angles in biomolecules by NMR in a dilute liquid crystalline medium. *Science*, 278(5340): 1111–1114, 1997.
- [10] K. Schmidt-Rohr, L. Emsley D. Nanz, and A. Pines. NMR measurement of resolved heteronuclear dipole couplings in liquid crystals and lipids. *J. Phys. Chem.*, 98: 6668, 1994.
- [11] S. Caldarelli, M. Hong, L. Emsley, and A. Pines. Measurement of carbon-proton dipolar couplings in liquid crystals by local dipolar field NMR spectroscopy. *J. Phys. Chem.*, 100: 18696, 1996.
- [12] P. Lesot, J. M. Ouvrard, B. N. Ouvrard, and J. Courtieu. Coherent reduction of dipolar interactions in molecules dissolved in anisotropic media using a new multiple-pulse sequence in a COSY experiment. *J. Magn. Reson. A*, 107: 141–150, 1994.
- [13] W. K. Rhim, D. D. Elleman, and R. W. Vaughan. Analysis of multiple pulse NMR in solids. *J. Chem. Phys.*, 59(7): 3740, 1973.
- [14] J. Courtieu, D. W. Alderman, and D. M. Grant. Spinning near the magic angle: A means of obtaining first-order dipolar NMR spectra of molecules dissolved in nematic liquid crystals. *J. Am. Chem. Soc.*, 103: 6783–6784, 1981.

- [15] J. Courtieu, D. W. Alderman, D. M. Grant, and J. P. Bayle. Director dynamics and NMR applications of nematic liquid crystals spinning at various angles from the magnetic field. *J. Chem. Phys.*, 77: 723–730, 1982.
- [16] J. Courtieu, J. P. Bayle, and B. M. Fung. Variable angle sample spinning NMR in liquid crystals. *Prog. Nucl. Magn. Reson. Spectrosc.*, 26: 141–169, 1994.
- [17] R. H. Havlin, G. H. J. Park, and A. Pines. Two-dimensional NMR correlations of liquid crystals using switched angle spinning. *J. Magn. Reson.*, 157: 163–169, 2002.
- [18] G. Zandomeneghi, M. Tomaselli, J.D. van Beek, and B.H. Meier. Manipulation of the director in bicellar mesophases by sample spinning: A new tool for NMR spectroscopy. *J. Am. Chem. Soc.*, 123: 910, 2001.
- [19] D. McElheny, M. Zhou, and L. Frydman. Two-dimensional dynamic-director ^{13}C NMR in liquid crystals. *J. Magn. Reson.*, 148: 436–441, 2001.
- [20] A. Bax, N. M. Szeverenyi, and G. E. Maciel. Chemical-shift anisotropy in powdered solids studied by 2D FT NMR with flipping of the spinning axis. *J. Magn. Reson.*, 55(3): 494–497, 1983.
- [21] T. Terao, H. Miura, and A. Saika. Dipolar SASS NMR-spectroscopy - separation of heteronuclear dipolar powder patterns in rotating solids. *J. Chem. Phys.*, 85(7): 3816–3826, 1986.
- [22] G. Zandomeneghi, P. T. F. Williamson, A. Hunkeler, and B. H. Meier. Switched-angle spinning applied to bicelles containing phospholipid-associated peptides. *J. Biomol. NMR*, 25(2): 125–132, 2003.

- [23] L. Emsley and A. Pines. *Proceedings of the International School of Physics*. Societa Italiana di Fisica, 1994.
- [24] C. Algieri, F. Castiglione, G. Celebre, G. De Luca, M. Longeri, and J. W. Emsley. The structure of ethylbenzene as a solute in liquid crystalline solvents via analysis of proton NMR spectra. *Phys. Chem. Chem. Phys.*, 2: 3405–3413, 2000.
- [25] W. Maier and A. Saupe. *Z. Naturforsch. A*, 14: 882, 1959.
- [26] W. Maier and A. Saupe. *Z. Naturforsch. A*, 15: 287, 1960.
- [27] R. Fields, J. Lee and D. J. Mowthorpe. *J. Chem. Soc. (B)*, 308-312, 1968.
- [28] U. Finkenzeller, T. Geelhaar, G. Weber, and L. Pohl. Liquid-crystalline reference compounds. *Liq. Cryst.*, 5(1): 313–321, 1989.
- [29] M. Mehring. *Principles of High Resolution NMR in Solids*. Springer-Verlag, New York, 2nd edition, 1983.
- [30] J. P. Bayle, A. Khandarshahabad, P. Gonord, and J. Courtieu. Nematic Director Dynamics Upon Macroscopic Rotation In A Magnetic-Field - Orientational Behavior Near The Magic Angle. *J. Chim. Phys. Physicochim. Biol.*, 83(3): 177–183, 1986.
- [31] B. S. Arun Kumar, K. V. Ramanathan, and C. L. Khetrapal. Side-Band Intensities In The Deuteium Magnetic Resonance Spectra Of Oriented Molecules Spinning Near The Magic Angle. *Chem. Phys. Lett.*, 149(3): 306–309, 1988.
- [32] J. Herzfeld and A. E. Berger. Sideband intensities in NMR-spectra of samples spinning at the magic angle. *J. Chem. Phys.*, 73(12): 6021–6030, 1980.

- [33] M. Lee and W. Goldburg. Nuclear-magnetic-resonance line narrowing by a rotating RF field. *Phys. Rev.*, 140: 1261–1271, 1965.
- [34] A. C. deDios and E. Oldfield. Recent progress in understanding chemical shifts. *Solid State NMR*, 6(2): 101–125, 1996.
- [35] R. H. Havlin, H. Le, D. D. Laws, A. C. deDios, and E. Oldfield. An ab initio quantum chemical investigation of carbon-13 NMR shielding tensors in glycine, alanine, valine, isoleucine, serine, and threonine: Comparisons between helical and sheet tensors, and the effects of Chi-1 on shielding. *J. Am. Chem. Soc.*, 119(49): 11951–11958, 1997.
- [36] R. H. Havlin, D. D. Laws, H. M. L. Bitter, L. K. Sanders, H. Sun, J. S. Grimley, D. E. Wemmer, A. Pines, , and E. Oldfield. An experimental and theoretical investigation of the chemical shielding tensors of $(^{13}\text{C}(\alpha))$ of alanine, valine, and leucine residues in solid peptides and in proteins in solution. *J. Am. Chem. Soc.*, 123(42): 10362–10369, 2001.
- [37] G. Zandomenoghi, M. Tomaselli, P. T. F. Williamson, and B. H. Meier. NMR of bicelles: orientation and mosaic spread of the liquid-crystal director under sample rotation *J. Biomol. NMR*, 25(2): 113–123, 2003.

